Computing Upper and Lower Bounds for the J-Integral in Two-Dimensional Linear Elasticity

Z.C. Xuan*, K.H. Lee*†, A.T. Patera*‡, J. Peraire*§

*Singapore-MIT Alliance
†Department of Mechanical Engineering, National University of Singapore
‡Department of Mechanical Engineering, Massachusetts Institute of Technology
§Department of Aeronautics and Astronautics, Massachusetts Institute of Technology

(This paper is dedicated to the memory of Kwok Hong Lee)

***Abstract*— We present an *a-posteriori* method for computing rigorous upper and lower bounds of the J-integral in two dimensional linear elasticity. The J-integral, which is typically expressed as a contour integral, is recast as a surface integral which yields a quadratic continuous functional of the displacement. By expanding the quadratic output about an approximate finite element solution, the output is expressed as a known computable quantity plus linear and quadratic functionals of the solution error. The quadratic component is bounded by the energy norm of the error scaled by a continuity constant, which is determined explicitly. The linear component is expressed as an inner product of the errors in the displacement and in a computed adjoint solution, and bounded using standard a-posteriori error estimation techniques. The method is illustrated with two fracture problems in plane strain elasticity.**

I. Introduction

The accurate prediction of stress intensity factors in crack tips is essential for assessing the strength and life of structures using linear fracture mechanics theories. A crack is assumed to be stable when the magnitude of the stress concentration at its tip is below a critical material dependent value. Stress intensity factors derived from linearly elastic solutions are widely used in the study of brittle fracture, fatigue, stress corrosion cracking, and to some extend for creep crack growth. Since the analytical methods for solving the equations of elasticity are limited to very simple cases, the finite element method is commonly used as the alternative to treat the more complicated cases. The methods for extracting stress intensity factors from computed displacement solutions fall into two categories: displacement matching methods, and the energy based methods. In the first case, the form of the local solution is assumed, and the value of the displacement near crack tip is used to determine the magnitude of the coefficients in the asymmptotic expansion. In the second case, the strength of the singular stress field is related to the energy released rate, i.e. the sensitivity of the total potential energy to the crack position. An expression for calculating the energy release rate in two dimensional cracks was given in [13] and is known as the J-integral. The J-integral is a path independent contour integral involving the projection of the material force derived from Eshelby's [3] energy momentum tensor along the direction of the possible crack extension. An alternative form of the J-integral in which the contour integral is transformed into a domain integral involving a suitably defined weighting function is given in [6]. The expression for the energy release rate given in [6] appears to be very versatile and has an easier and more convenient generalization to three dimensions than the original form [13].

Regardless of the method chosen to evaluate the stress intensity factor, a good approximation to the solution of the linear elasticity equations is required. Unfortunately, the problems of interest involve singularities and this makes the task of computing accurate solutions much harder. For instance, it is well known [16] that the convergence rate of energy norm of a standard finite element solution for a linear elasticity problem involving a 180^o reentrant corner is no higher than $O(H^{1/2})$, where H is the typical mesh size. This problem was soon realized and as a consequence a number of mesh adaptive algorithms have been proposed [4], [5], [7], [8], [14] which, in general, improve the situation considerably. In some cases [7], [8], the adaptivity is driven by errors in the energy norm of the solution, whereas in some others [4], [5], [14], a more sophisticated goal-oriented approach based on a linearized form of the output is used.

In this paper we present a method for computing strict upper and lower bounds for the value of the J-integral in two dimensional linear fracture mechanics. The J-integral is written as a bounded quadratic functional of the displacement and expanded into computable quantities plus additional linear and quadratic terms in the error. The linear terms are bounded using our previous work for linear functional outputs [9], [11], [12] and the quadratic term is bounded with the energy norm of the error scaled by a suitably chosen continuity constant, which can be determined a priori. The bounds produced are strict with respect to the solution that would be obtained on a conservatively refined reference mesh. This restriction however can be eliminated if the more rigorous techniques for bounding the outputs of the exact weak solutions are employed [10], [15]. Also, not exploited here, but of clear practical

interest, is the fact that the bound gap can be decomposed into a sum of positive elemental contributions thus naturally leading to an adaptive mesh adaptive approach [12]. We think that the algorithm presented is an attractive alternative to the existing methods as it guarantees the certainty of the computed bounds. This is particularly important in critical problems relating to structural failure. The method is illustrated for an open mode and a mixed mode crack examples.

II. Problem Formulation

We consider a linear elastic body occupying a region $\Omega \subset \mathbb{R}^2$. The boundary of Ω, $\partial\Omega$, is assumed to be piecewise smooth, and composed of a Dirichlet portion Γ_D, and a Neumann portion Γ_N, i.e. $\partial\Omega = \Gamma_D \cup \Gamma_N$. We assume that a traction $\boldsymbol{g} \in (H^{-1/2}(\Gamma_N))^2$ is applied on the Neumann boundary and that the Dirichlet boundary conditions are homogeneous. The displacement field $\boldsymbol{u} = (u_1, u_2) \in X \equiv \{\boldsymbol{v} = (v_1, v_2) \in (H^1(\Omega))^2 \mid \boldsymbol{v} = \boldsymbol{0} \text{ on } \Gamma_D\}$ satisfies the following weak form of the elasticity equations

$$a(\boldsymbol{u}, \boldsymbol{v}) = (\boldsymbol{f}, \boldsymbol{v}) + \langle \boldsymbol{g}, \boldsymbol{v} \rangle \,, \quad \forall \boldsymbol{v} \in X, \tag{1}$$

in which

$$(\boldsymbol{f}, \boldsymbol{v}) = \int_\Omega \boldsymbol{f} \cdot \boldsymbol{v} \, \mathrm{d}\Omega \,,$$
$$\langle \boldsymbol{g}, \boldsymbol{v} \rangle = \int_{\Gamma_N} \boldsymbol{g} \cdot \boldsymbol{v} \, \mathrm{d}\Gamma \,,$$

where $\boldsymbol{f} \in (H^{-1}(\Omega))^2$ is the body force. The bi-linear form $a(\boldsymbol{w}, \boldsymbol{v}) : X \times X \to \mathbb{R}$ is given by,

$$a(\boldsymbol{w}, \boldsymbol{v}) = \int_\Omega \boldsymbol{\sigma}(\boldsymbol{w}) : \boldsymbol{\varepsilon}(\boldsymbol{v}) \, \mathrm{d}\Omega \,. \tag{2}$$

Here, $\boldsymbol{\varepsilon}(\boldsymbol{v})$ denotes the second order deformation tensor which is defined as the symmetric part of the gradient tensor $\boldsymbol{\nabla v}$. That is, $\boldsymbol{\varepsilon}(\boldsymbol{v}) = (\boldsymbol{\nabla v} + (\boldsymbol{\nabla v})^T)/2$. The stress $\boldsymbol{\sigma}(\boldsymbol{v})$ is related to the deformation tensor through a linear constitutive relation of the form

$$\boldsymbol{\sigma}(\boldsymbol{v}) = \boldsymbol{C} : \boldsymbol{\varepsilon}(\boldsymbol{v}) \tag{3}$$

where $\boldsymbol{C}$ is the constant fourth-order elasticity tensor. We define the total potential energy functional $\Pi(\boldsymbol{v}) : X \to \mathbb{R}$ as

$$\Pi(\boldsymbol{v}) = \frac{1}{2} a(\boldsymbol{v}, \boldsymbol{v}) - (\boldsymbol{f}, \boldsymbol{v}) - \langle \boldsymbol{g}, \boldsymbol{v} \rangle \tag{4}$$

It is straightforward to see that the solution, $\boldsymbol{u}$, to the problem (1) minimizes the total potential energy, and that

$$\Pi(\boldsymbol{u}) = -\frac{1}{2} a(\boldsymbol{u}, \boldsymbol{u}) = -\frac{1}{2} |||\boldsymbol{u}|||^2 \,. \tag{5}$$

Where $|||\cdot||| = a(\cdot, \cdot)^{1/2}$ denotes energy norm associated with the coercive bilinear form $a(\cdot, \cdot)$.

In fracture mechanics we are often interested in determining the strength of the crack tip stress fields. A common way to do that is to relate the so called stress intensity factors to the energy released per unit length of crack advancement (see figure 1). If the total potential energy defined by (5), decreases by an amount $\delta\Pi(\boldsymbol{u})$ when the crack advances by a distance $\delta\ell$ in its plane, we are interested in determining the energy release rate, $J(\boldsymbol{u})$, such that,

$$\delta\Pi(\boldsymbol{u}) = -J(\boldsymbol{u})\delta\ell \,.$$

For a two-dimensional linear elastic body the energy release

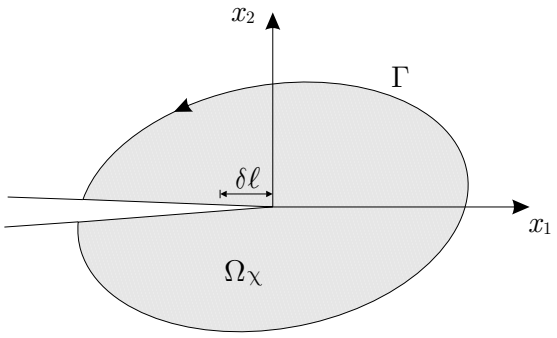

Fig. 1. Crack geometry showing coordinate axes and the J-integral contour and domain of integration.

rate, $J(\boldsymbol{u})$, can be calculated as a path independent line integral known as the J-integral [13]. If we consider the geometry shown in figure 1, the J-integral has the following expression,

$$J(\boldsymbol{u}) = \int_\Gamma \left(W^e n_1 - \boldsymbol{T} \cdot \frac{\partial \boldsymbol{u}}{\partial x_1} \right) \mathrm{d}\Gamma \,, \tag{6}$$

where Γ is any path beginning at the bottom crack face and ending at the top crack face, $W^e = (\boldsymbol{\sigma} : \boldsymbol{\varepsilon})/2$ is the strain energy density, $\boldsymbol{T}$ is the traction given as $\boldsymbol{T} = \boldsymbol{\sigma n}$, and $\boldsymbol{n} = (n_1, n_2)$ is the outward unit normal to Γ. An alternative expression for $J(\boldsymbol{u})$ was proposed in [6], where the contour integral is transformed to the following area integral expression,

$$J(\boldsymbol{u}) = \int_{\Omega_\chi} \left((\boldsymbol{\nabla}\chi)^T \cdot \boldsymbol{\sigma} \frac{\partial \boldsymbol{u}}{\partial x_1} - W^e \frac{\partial \chi}{\partial x_1} \right) \mathrm{d}\Omega. \tag{7}$$

Here, the weighting function χ is any function in $H^1(\Omega_\chi)$ that is equal to one at the crack tip and vanishes on Γ.

For a given χ, we observe that $J(\boldsymbol{u})$ is a bounded quadratic functional of $\boldsymbol{u}$. For our bounding procedure it is convenient to make the quadratic dependence of the output on the solution more explicit. To this end, we define the bilinear form $\bar{q}(\boldsymbol{w}, \boldsymbol{v}) : X \times X \to \mathbb{R}$ as,

$$\bar{q}(\boldsymbol{w}, \boldsymbol{v}) = \int_{\Omega_\chi} (\boldsymbol{\nabla}\chi)^T \cdot \boldsymbol{\sigma}(\boldsymbol{w}) \frac{\partial \boldsymbol{v}}{\partial x_1} \, \mathrm{d}\Omega - \int_{\Omega_\chi} \frac{1}{2} \boldsymbol{\sigma}(\boldsymbol{w}) : \boldsymbol{\varepsilon}(\boldsymbol{v}) \frac{\partial \chi}{\partial x_1} \, \mathrm{d}\Omega, \tag{8}$$

and its symmetric part $q(\boldsymbol{w}, \boldsymbol{v}) : X \times X \to \mathbb{R}$,

$$q(\boldsymbol{w}, \boldsymbol{v}) = \frac{1}{2} (\bar{q}(\boldsymbol{w}, \boldsymbol{v}) + \bar{q}(\boldsymbol{v}, \boldsymbol{w})) \,. \tag{9}$$

It is clear from these definitions that,

$$J(\boldsymbol{u}) = q(\boldsymbol{u}, \boldsymbol{u}) \,, \tag{10}$$

and that there exists $\eta < \infty$ such that,

$$q(\boldsymbol{v},\boldsymbol{v}) \le \eta |||\boldsymbol{v}|||^2 , \qquad \forall \boldsymbol{v} \in X. \tag{11}$$

III. Bounding Procedure

Our objective is to compute upper and lower bounds, for $J(\boldsymbol{u})$, where $\boldsymbol{u}$ satisfies problem (1). Let us consider a finite element approximation $\boldsymbol{u}_H \in X_H$ satisfying

$$a(\boldsymbol{u}_H,\boldsymbol{v}) = (\boldsymbol{f},\boldsymbol{v}) + \langle \boldsymbol{g},\boldsymbol{v}\rangle , \quad \forall \boldsymbol{v} \in X_H . \tag{12}$$

Here, $X_H \subset X$ is a finite dimensional subspace of X. For simplicity, we shall assume that X_H is the space of piecewise linear continuous functions defined over a triangulation, $\mathcal{T}_H$, of Ω which satisfies the Dirichlet boundary conditions. An approximation to $J(\boldsymbol{u})$, J_H, can be obtained as

$$J_H = q(\boldsymbol{u}_H,\boldsymbol{u}_H) ,$$

where, for convenience, χ in (7) is chosen to be piecewise linear over the elements $T_H \in \mathcal{T}_H$. Exploiting the bi-linearity of $q(\boldsymbol{w},\boldsymbol{v})$, we can write

$$\begin{aligned} J(\boldsymbol{u}) - J_H &= q(\boldsymbol{u},\boldsymbol{u}) - q(\boldsymbol{u}_H,\boldsymbol{u}_H) \\ &= q(\boldsymbol{u}-\boldsymbol{u}_H,\boldsymbol{u}-\boldsymbol{u}_H) + 2q(\boldsymbol{u},\boldsymbol{u}_H) - 2q(\boldsymbol{u}_H,\boldsymbol{u}_H) \\ &= q(\boldsymbol{e},\boldsymbol{e}) + 2q(\boldsymbol{e},\boldsymbol{u}_H) , \end{aligned} \tag{13}$$

where $\boldsymbol{e} = \boldsymbol{u} - \boldsymbol{u}_H$ is the error in the approximation $\boldsymbol{u}_H$. It is clear that if we are able to compute bounds Q and $L^{\pm}$ for the quadratic and linear error terms,

$$|q(\boldsymbol{e},\boldsymbol{e})| \le Q$$

and

$$L^- \le q(\boldsymbol{e},\boldsymbol{u}_H) \le L^+,$$

then, the bounds for $J(\boldsymbol{u})$, $J^{\pm}$, follow as,

$$J^- \equiv J_H - Q + 2L^- \le J(\boldsymbol{u}) \le J_H + Q + 2L^+ \equiv J^+ .$$

A. Linear term

In order to derive upper an lower bounds for the linear term $q(\boldsymbol{e},\boldsymbol{u}_H)$, we introduce the following adjoint problem: find $\boldsymbol{\psi} \in X$ such that

$$a(\boldsymbol{v},\boldsymbol{\psi}) = q(\boldsymbol{v},\boldsymbol{u}_H) , \quad \forall \boldsymbol{v} \in X , \tag{14}$$

and the corresponding finite element approximation, $\boldsymbol{\psi}_H \in X_H \subset X$, such that

$$a(\boldsymbol{v},\boldsymbol{\psi}_H) = q(\boldsymbol{v},\boldsymbol{u}_H) , \quad \forall \boldsymbol{v} \in X_H . \tag{15}$$

From (1) and (12), it follows that $a(\boldsymbol{e},\boldsymbol{v}) = 0$ for all $\boldsymbol{v} \in X_H$. In particular, $a(\boldsymbol{e},\boldsymbol{\psi}_H) = 0$. This, combined with the above equations (14) and (15) gives the following representation for the linear error term,

$$q(\boldsymbol{e},\boldsymbol{u}_H) = a(\boldsymbol{e},\boldsymbol{\epsilon}) , \tag{16}$$

where $\boldsymbol{\epsilon} = \boldsymbol{\psi} - \boldsymbol{\psi}_H$ is the error in the adjoint solution. Now, using the parallelogram identity, we have that for all $\alpha \in \mathbb{R}$,

$$a(\boldsymbol{e},\boldsymbol{\epsilon}) = \frac{1}{4}|||\alpha\,\boldsymbol{e} + \frac{1}{\alpha}\boldsymbol{\epsilon}|||^2 - \frac{1}{4}|||\alpha\,\boldsymbol{e} - \frac{1}{\alpha}\boldsymbol{\epsilon}|||^2 , \tag{17}$$

and therefore,

$$-\frac{1}{4}|||\alpha\,\boldsymbol{e} - \frac{1}{\alpha}\boldsymbol{\epsilon}|||^2 \le q(\boldsymbol{e},\boldsymbol{u}_H) \le \frac{1}{4}|||\alpha\,\boldsymbol{e} + \frac{1}{\alpha}\boldsymbol{\epsilon}|||^2 . \tag{18}$$

B. Quadratic term

In the appendix we show that for two dimensional linear elasticity, a suitable value for the continuity constant in expression (11) is given by

$$\eta_\chi = \max_{T_H \in \mathcal{T}_H} \frac{(3\kappa+4\mu)|\boldsymbol{\nabla}\chi|^2}{4\sqrt{(3\kappa+\mu)\left(3\mu\left(\frac{\partial\chi}{\partial x_1}\right)^2 + (3\kappa+4\mu)\left(\frac{\partial\chi}{\partial x_2}\right)^2\right)}} , \tag{19}$$

where $\mu = E/(2(1+\nu))$ is the elastic shear modulus, κ is the elastic bulk modulus which is given by $\kappa = E/(1+2\nu)/(3(1-\nu^2))$ for plane stress, and $\kappa = E/(3(1-2\nu))$ for plain strain. In these expressions, E is Young's elastic modulus and ν is the Poisson's ratio. Therefore, we write

$$q(\boldsymbol{e},\boldsymbol{e}) \le \eta_\chi |||\boldsymbol{e}|||^2 .$$

The computation of a bound for $q(\boldsymbol{e},\boldsymbol{e})$ is straightforward once a bound for the error in the energy norm $|||\boldsymbol{e}|||$ has been obtained.

IV. Bounds for energy norm of the error

An essential ingredient for the computation of the bounds for our output of interest, $J(\boldsymbol{u})$, is the calculation of upper bounds for the energy norm of $\boldsymbol{e}$, and $\alpha\boldsymbol{e} \pm \boldsymbol{\epsilon}/\alpha$. There is an extensive body of literature on this subject (see [1], [11]), and a number of methods an approaches have been proposed which, in principle, would be applicable here. These methods typically compute an upper bound of the energy norm of the error measured with respect to a reference solution. This reference solution can be a finite element solution obtained on a very fine mesh or a solution obtained using a high degree interpolation polynomial. More recently, a method was proposed in [15] for Poisson's equation which is based on the use of the complementary energy principle and gives bounds for the error relative to the exact weak solution. The method has been since generalized to the linear elasticity equations in [10]. Here, we will use essentially the method proposed in [2] for Poisson's equation, extended to the linear elasticity problem. This approach is easy to implement but has the disadvantage that the error in the solution is measured with respect to the finite element solution obtained on a conservatively refined mesh. Future work will incorporate the more rigorous bounding procedures described in [10].

We start by combining equations (1) and (12) to write an equation for the error,

$$a(\boldsymbol{e},\boldsymbol{v}) = (\boldsymbol{f},\boldsymbol{v}) + \langle \boldsymbol{g},\boldsymbol{v}\rangle - a(\boldsymbol{u}_H,\boldsymbol{v}) \equiv \mathcal{R}(\boldsymbol{v}) , \quad \forall \boldsymbol{v} \in X \tag{20}$$

where $\mathcal{R}(\boldsymbol{v}) : X \to \mathbb{R}$ is the residual. Next, we introduce the "broken" space $\hat{X} \subset X$, supported by the triangulation $\mathcal{T}_H$,

$$\hat{X} = \{\boldsymbol{v} \,|\, \boldsymbol{v} \in (H^1(T_H))^2,\ \forall T_H \in \mathcal{T}_H, \boldsymbol{v} = \boldsymbol{0} \text{ on } \Gamma_D\} , \tag{21}$$

where T_H denotes a typical triangle of $\mathcal{T}_H$ with boundary ∂T_H. We can then extend the bi-linear form $a(\boldsymbol{w},\boldsymbol{v})$ and the residual $\mathcal{R}(\boldsymbol{v})$ to admit functions which are discontinuous across triangles. We define

$$a_{T_H}(\boldsymbol{w},\boldsymbol{v}) = \int_{T_H} \boldsymbol{\sigma}(\boldsymbol{w}) : \varepsilon(\boldsymbol{v})\,\mathrm{d}\Omega \tag{22}$$

$$\mathcal{R}_{T_H}(\boldsymbol{v}) = \int_{T_H} \boldsymbol{f}\cdot\boldsymbol{v}\,\mathrm{d}\Omega + \int_{\partial T_H\cap\Gamma_N} \boldsymbol{g}\cdot\boldsymbol{v}\,\mathrm{d}\Gamma - a_{T_H}(\boldsymbol{u}_H,\boldsymbol{v})\ . \tag{23}$$

and write,

$$a(\boldsymbol{w},\boldsymbol{v}) = \sum_{T_H\in\mathcal{T}_H} a_{T_H}(\boldsymbol{w},\boldsymbol{v}) \tag{24}$$

$$\mathcal{R}(\boldsymbol{v}) = \sum_{T_H\in\mathcal{T}_H} \mathcal{R}_{T_H}(\boldsymbol{v})\ . \tag{25}$$

Substituting $\boldsymbol{u} = \boldsymbol{e}+\boldsymbol{u}_H$ on element T_H into the governing equations, $-\boldsymbol{\nabla}\cdot\boldsymbol{\sigma}(\boldsymbol{u}) = \boldsymbol{f}$, we find that, on T_H, the error $\boldsymbol{e}$ satisfies the differential equation

$$-\boldsymbol{\nabla}\cdot\boldsymbol{\sigma}(\boldsymbol{e}) = \boldsymbol{f} + \boldsymbol{\nabla}\cdot\boldsymbol{\sigma}(\boldsymbol{u}_H). \tag{26}$$

Multiplying both sides of the local error equation (26) by $\boldsymbol{v}\in\hat{X}$, and performing integration by parts using Green's formula leads to the weak form of the error residual differential equation over a triangle

$$a_{T_H}(\boldsymbol{e},\boldsymbol{v}) = \mathcal{R}_{T_H}(\boldsymbol{v}) + \langle\boldsymbol{\sigma}(u)\cdot\boldsymbol{n}_{T_H},\boldsymbol{v}\rangle_{\partial T_H\cap\mathcal{E}_I}\ ,\ \forall\boldsymbol{v}\in\hat{X}. \tag{27}$$

Here, $\mathcal{E}_I$ is the set of all edges in the triangulation $\mathcal{T}_H$ excluding those on Γ_N, and $\boldsymbol{n}_{T_H}$ is the outward unit normal to ∂T_H.

By approximating the normal traction $\boldsymbol{\sigma}(\boldsymbol{u})\cdot\boldsymbol{n}_{T_H}$ by the traction computed by averaging the traction $\boldsymbol{\sigma}(\boldsymbol{u}_H)$ on the two neighboring elements [1], that is,

$$\boldsymbol{\sigma}(\boldsymbol{u})\cdot\boldsymbol{n}_{T_H} \approx \bar{\boldsymbol{\sigma}}(\boldsymbol{u}_H)\cdot\boldsymbol{n}_{T_H} = \frac{1}{2}\left(\boldsymbol{\sigma}(\boldsymbol{u}_H)|^{+}_{\partial T_H} + \boldsymbol{\sigma}(\boldsymbol{u}_H)|^{-}_{\partial T_H}\right)\cdot\boldsymbol{n}_{T_H},$$

we can write the following problem for the approximate local error $\hat{\boldsymbol{e}}\in\hat{X}$ over each element T_H,

$$a_{T_H}(\hat{\boldsymbol{e}},\boldsymbol{v}) = \mathcal{R}_{T_H}(\boldsymbol{v}) + \langle\bar{\boldsymbol{\sigma}}(\boldsymbol{u}_H)\cdot\boldsymbol{n}_{T_H},\boldsymbol{v}\rangle_{\partial T_H\cap\mathcal{E}_I}\ ,\ \forall\boldsymbol{v}\in\hat{X}. \tag{28}$$

In general, the above local problems are not solvable. A common way to fix this problem is to solve instead the modified local problems [2],

$$a_{T_H}(\hat{\boldsymbol{e}},\boldsymbol{v}) = \mathcal{R}_{T_H}(\boldsymbol{v}-\mathcal{I}_H\boldsymbol{v}) + \langle\bar{\boldsymbol{\sigma}}(\boldsymbol{u}_H)\cdot\boldsymbol{n}_{T_H},\boldsymbol{v}-\mathcal{I}_H\boldsymbol{v}\rangle_{\partial T_H\cap\mathcal{E}_I},\forall\boldsymbol{v}\in\hat{X}_h, \tag{29}$$

in which $\mathcal{I}_H(\boldsymbol{v}):\hat{X}\to\hat{X}_H$ denotes the nodal interpolation operator. Thus, we have that if $\boldsymbol{v}\in\hat{X}$, then, $\mathcal{I}_H\boldsymbol{v}\in\hat{X}_H$, and if $\boldsymbol{v}\in$, then, $\hat{X}_H$, $\mathcal{I}_H\boldsymbol{v}=\boldsymbol{v}$. Problem (29) is local over each element but is still infinite dimensional. In practice, we discretize (29) over a conservatively fine mesh and compute an approximation, $\hat{\boldsymbol{e}}_h$, to $\hat{\boldsymbol{e}}$ (see [1], [2], or [11] for details). We shall assume here that the discretization is sufficiently rich so that the difference between $a(\hat{\boldsymbol{e}}_h,\hat{\boldsymbol{e}}_h)$ and $a(\hat{\boldsymbol{e}},\hat{\boldsymbol{e}})$ is negligible.

Summing the elemental equations (29) over all the elements in $\mathcal{T}_H$, and letting $\boldsymbol{v}=\boldsymbol{e}$ leads to,

$$a(\hat{\boldsymbol{e}},\boldsymbol{e}) = \mathcal{R}(\boldsymbol{e}) - \mathcal{R}(\mathcal{I}_H\boldsymbol{e}) + \sum_{T_H\in\mathcal{T}_H}\langle\bar{\boldsymbol{\sigma}}(\boldsymbol{u}_H)\cdot\boldsymbol{n}_{T_H},\boldsymbol{e}-\mathcal{I}_H\boldsymbol{e}\rangle_{\partial T_H\cap\mathcal{E}_I}\ . \tag{30}$$

Since $\mathcal{I}_H\boldsymbol{e}\in X_H$, $\mathcal{R}(\mathcal{I}_H\boldsymbol{e})=0$, and

$$\bar{\boldsymbol{\sigma}}(\boldsymbol{u}_H)\cdot\boldsymbol{n}_{T_H} = -\bar{\boldsymbol{\sigma}}(\boldsymbol{u}_H)\cdot\boldsymbol{n}_{T'_H} \tag{31}$$

on the common edge $\partial T_H = \partial T'_H\in\mathcal{E}_I$ of the two neighbor elements, the last term in the right hand side is also zero. This yields,

$$a(\hat{\boldsymbol{e}},\boldsymbol{e}) = \mathcal{R}(\boldsymbol{e}) = a(\boldsymbol{e},\boldsymbol{e}). \tag{32}$$

The last equality follows from (20) with $\boldsymbol{v}=\boldsymbol{e}$. Finally since $a(\boldsymbol{e}-\hat{\boldsymbol{e}},\boldsymbol{e}-\hat{\boldsymbol{e}})\geq 0$, from the above expression, it follows the desired result,

$$a(\boldsymbol{e},\boldsymbol{e})\leq a(\hat{\boldsymbol{e}},\hat{\boldsymbol{e}}),\quad\text{or}\quad |||\boldsymbol{e}|||\leq|||\hat{\boldsymbol{e}}|||\ . \tag{33}$$

If we now start with the adjoint error equation,

$$a(\boldsymbol{v},\boldsymbol{\epsilon}) = q(\boldsymbol{v},\boldsymbol{u}_H) - a(\boldsymbol{v},\boldsymbol{\psi}_H) \equiv \mathcal{R}^*(\boldsymbol{v})\ , \tag{34}$$

and repeat the same process outlined above, we can determine a reconstructed adjoint error $\hat{\boldsymbol{\epsilon}}$ satisfying,

$$a(\boldsymbol{\epsilon},\boldsymbol{\epsilon})\leq a(\hat{\boldsymbol{\epsilon}},\hat{\boldsymbol{\epsilon}}),\quad\text{or}\quad |||\boldsymbol{\epsilon}|||\leq|||\hat{\boldsymbol{\epsilon}}|||\ . \tag{35}$$

Finally, we note that due to the symmetry of $a(\cdot,\cdot)$, equations (20) and (34) can be combined into the following equation,

$$a(\alpha\boldsymbol{e}\pm\frac{1}{\alpha}\boldsymbol{\epsilon},\boldsymbol{v}) = \alpha\mathcal{R}(\boldsymbol{v})\pm\frac{1}{\alpha}\mathcal{R}^*(v)\ , \tag{36}$$

and an upper bound for the norm of the combined error is thus,

$$|||\alpha\boldsymbol{e}\pm\frac{1}{\alpha}\boldsymbol{\epsilon}|||\leq\alpha^2|||\hat{\boldsymbol{e}}|||\pm 2a(\hat{\boldsymbol{e}},\hat{\boldsymbol{\epsilon}})+\frac{1}{\alpha^2}|||\hat{\boldsymbol{\epsilon}}|||\ . \tag{37}$$

Since α in equation (18) is arbitrary we choose $\alpha^2 = |||\hat{\boldsymbol{\epsilon}}|||/|||\hat{\boldsymbol{e}}|||$ to obtain,

$$2a(\hat{\boldsymbol{e}},\hat{\boldsymbol{\epsilon}})-2|||\hat{\boldsymbol{e}}|||\,|||\hat{\boldsymbol{\epsilon}}|||\leq q(\boldsymbol{e},\boldsymbol{u}_H)\leq 2a(\hat{\boldsymbol{e}},\hat{\boldsymbol{\epsilon}})+2|||\hat{\boldsymbol{e}}|||\,|||\hat{\boldsymbol{\epsilon}}|||\ . \tag{38}$$

V. Summary of the bounds procedure

We summarize here the steps involved in the implementation of the bounds procedure.

STEP 1: Solve a global problem for the approximate displacement field $\boldsymbol{u}_H$: find $\boldsymbol{u}_H\in X_H$ such that

$$a(\boldsymbol{u}_H,\boldsymbol{v}) = (\boldsymbol{f},\boldsymbol{v}) + \langle\boldsymbol{g},\boldsymbol{v}\rangle\ ,\ \forall\boldsymbol{v}\in X_H\ ,$$

and determine $J_H = J(\boldsymbol{u}_H)$.

STEP 2: Solve a global problem for the approximate adjoint solution $\boldsymbol{\psi}_H$: find $\boldsymbol{\psi}_H\in X_H$ such that

$$a(\boldsymbol{v},\boldsymbol{\psi}_H) = q(\boldsymbol{v},\boldsymbol{u}_H),\ \forall\boldsymbol{v}\in X_H\ .$$

STEP 3: Solve for each element $T_H \in \mathcal{T}_H$ a local problem for the reconstructed displacement $\hat{\boldsymbol{e}}$: find $\hat{\boldsymbol{e}}_h \in \hat{X}_h$ such that

$$a_{T_H}(\hat{\boldsymbol{e}_h}, \boldsymbol{v}) = \mathcal{R}_{T_H}(\boldsymbol{v} - \mathcal{I}_H \boldsymbol{v}) + \langle \bar{\boldsymbol{\sigma}}(\boldsymbol{u}_H) \cdot \boldsymbol{n}_{T_H}, \boldsymbol{v} - \mathcal{I}_H \boldsymbol{v} \rangle_{\partial T_H \cap \mathcal{E}_I}, \ \forall \boldsymbol{v} \in \hat{X}_h \ .$$

STEP 4: Solve for each element $T_H \in \mathcal{T}_H$ a local problem for the reconstructed adjoint error $\hat{\boldsymbol{\epsilon}}$: find $\hat{\boldsymbol{\epsilon}}_h \in \hat{X}_h$ such that

$$a_{T_H}(\boldsymbol{v}, \hat{\boldsymbol{\epsilon}}_h) = \mathcal{R}^*_{T_H}(\boldsymbol{v} - \mathcal{I}_H \boldsymbol{v}) + \langle \bar{\boldsymbol{\sigma}}(\boldsymbol{\psi}_H) \cdot \boldsymbol{n}_{T_H}, \boldsymbol{v} - \mathcal{I}_H \boldsymbol{v} \rangle_{\partial T_H \cap \mathcal{E}_I}, \ \forall \boldsymbol{v} \in \hat{X}_h \ .$$

STEP 5: Calculate $|||\hat{\boldsymbol{e}}_h||| = [a(\hat{\boldsymbol{e}}_h, \hat{\boldsymbol{e}}_h)]^{1/2}$, $|||\hat{\boldsymbol{\epsilon}}_h||| = [a(\hat{\boldsymbol{\epsilon}}_h, \hat{\boldsymbol{\epsilon}}_h)]^{1/2}$, and $a(\hat{\boldsymbol{e}}_h, \hat{\boldsymbol{\epsilon}}_h)$, and determine J^+ and J^- as,

$$J^+ = J_H + \eta |||\boldsymbol{e}_h|||^2 + a(\hat{\boldsymbol{e}}_h, \hat{\boldsymbol{\epsilon}}_h) + |||\hat{\boldsymbol{e}}_h||| \, |||\hat{\boldsymbol{\epsilon}}_h||| \tag{39}$$

$$J^- = J_H - \eta |||\boldsymbol{e}_h|||^2 + a(\hat{\boldsymbol{e}}_h, \hat{\boldsymbol{\epsilon}}_h) - |||\hat{\boldsymbol{e}}_h||| \, |||\hat{\boldsymbol{\epsilon}}_h||| \ . \tag{40}$$

VI. Examples

In the first example we consider a plate with two edge cracks subjected to a uniformly distributed tensile stress as shown in figure 2. The plate is assumed to be in plane strain. The value of the tensile force acting on the two ends of the plate is $p = 1$ and the dimension of the crack is $a = 5$. The non-dimensionalized Young's modulus is 1.0 and the Poisson's ratio is 0.3. The analytical value of the mode-I normalized stress intensity factor $\mathcal{K}_{\rm I}$ for the problem has been determined in [7] to be $\mathcal{K}_{\rm I}/(p\sqrt{\pi a}) = 1.16279$. Therefore, the exact value of the J-integral is obtained as $J_{exact} = (1-\nu^2)\mathcal{K}_{\rm I}^2/E = 19.3270$.

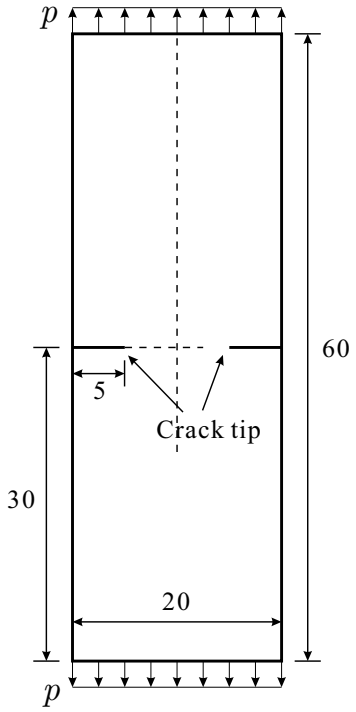

Fig. 2. Geometry of a double edge-cracked plate subjected to a uniform tensile stress.

Due to the symmetry of the problem, we only use one quarter of the plate for the finite element analysis. We use a 5 by 5 square area surrounding the crack tip as the support, Ω_χ, of the weighting function χ (see figure 3). Figure 4 shows three of the linear triangular meshes used for the global computations together with an illustration of the broken mesh used for the local Neumman problems. For all the calculations the reference mesh is taken to be a 32 refinement of the original coarse mesh $\mathcal{T}_H$. The value of the output on the reference mesh is 19.4246 which still has a relative error with respect to the exact solution of about 0.5%.

Table I shows the results for the output J_H, the norms of the reconstructed errors, and the computed upper and lower bounds, $J^{\pm}$, for J. The observed convergence rate of the bound gap is somewhat higher than the expected value of 1. We note that in the table I, all the results shown have been multiplied by two since, due to symmetry, only half of the domain is considered.

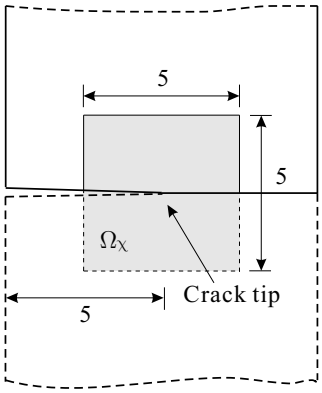

Fig. 3. Support of weighting function χ for the evaluation of the J-integral.

TABLE I
Bound results

Coarse mesh size	H	$H/2$	$H/4$	$H/8$	$H/16$
J_H	15.3666	17.4156	18.4982	19.0412	19.2982
$\eta a(\hat{e}, \hat{e})$	17.8458	5.6043	1.6175	0.4904	0.1325
$\|\|\|\hat{e}\|\|\|$	8.9780	5.0312	2.7029	1.4882	0.7736
$\|\|\|\hat{\epsilon}\|\|\|$	2.9814	2.2908	1.5467	0.9435	0.5286
J^-	-22.3265	2.3256	13.3991	17.3846	18.8259
J^+	66.8985	36.5854	24.9949	21.1736	19.9087

In the second example we consider a plate with an inclined crack subjected to a uniformly distributed tensile stress as shown in figure 5. The plate is assumed to be in plane strain. The value of the tensile force acting on the two ends of the plate is $p = 1$. The non-dimensionalized Young's modulus is 1.0 and the Poisson's ratio is 0.3. The analytical value of the mode-I and node-II normalized stress intensity factors, $\mathcal{K}_{\rm I}$ and $\mathcal{K}_{\rm II}$, for the problem have been determined in [7] to be $\mathcal{K}_{\rm I}/(p\sqrt{\pi a}) = 0.6611$ and $\mathcal{K}_{\rm II}/(p\sqrt{\pi a}) = 0.5674$, respectively. Therefore, the exact value of the J-integral is obtained as $J_{exact} = (1-\nu^2)(\mathcal{K}_{\rm I}^2 + \mathcal{K}_{\rm II}^2)/E = 6.3183$.

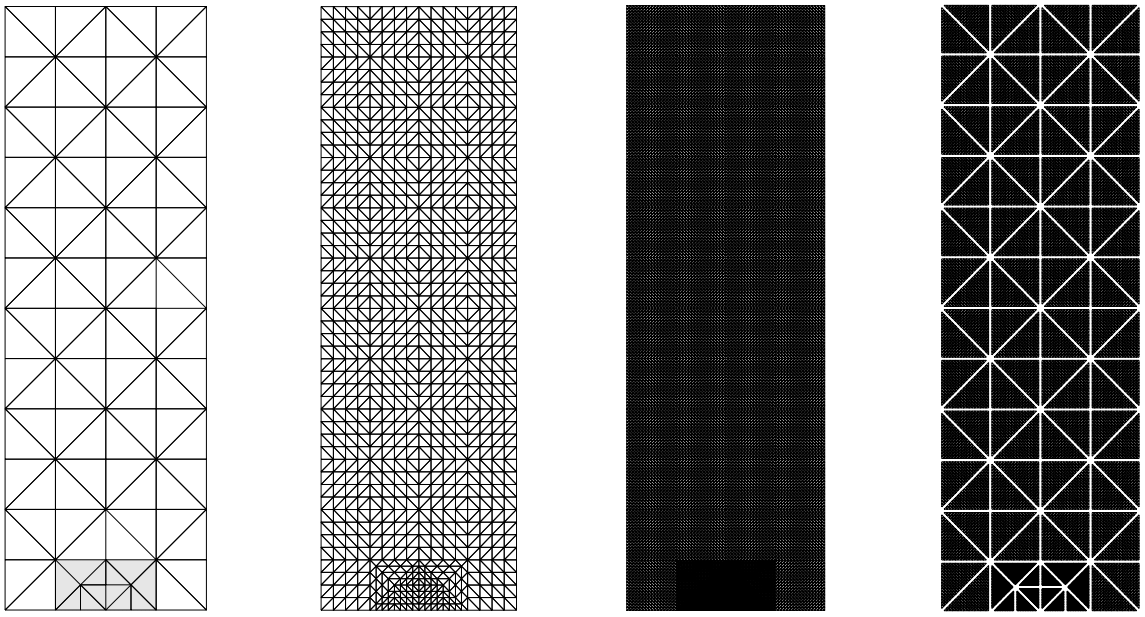

(a) (b) (c) (d)

Fig. 4. Finite element meshes used for open crack problem: (a) coarse mesh $\mathcal{T}_H$, (b) medium mesh $\mathcal{T}_{H/4}$, (c) fine mesh $\mathcal{T}_{H/16}$, and (d) illustration of broken mesh used for local problem solution associated to coarse mesh $\mathcal{T}_H$ (actual mesh is twice as fine e.g. $H/32$).

We use a 3 by 3 square area surrounding the crack tip as the support, Ω_χ, of the weighting function χ (see figure 6). Figure 7 shows three of the linear triangular meshes used for the global computations together with an illustration of the broken mesh used for the local Neumman problems. For all the calculations the reference mesh is taken to be a 32 refinement of the original coarse mesh $\mathcal{T}_H$. The value of the output on the reference mesh is 6.2301 which has a relative error with respect to the exact solution of about 1.4%.

Table II shows the results for the output J_H, the norms of the reconstructed errors, and the computed upper and lower bounds, $J^{\pm}$, for J.

TABLE II
BOUND RESULTS

Coarse mesh size	H	$H/2$	$H/4$	$H/8$	$H/16$
J_H	4.1722	5.3889	5.9313	6.1325	6.2034
$\eta a(\hat{e},\hat{e})$	10.7902	3.4107	0.8012	0.1829	0.0411
$\|\|\|\hat{e}\|\|\|$	6.4310	3.6156	1.7524	0.8373	0.3971
$\|\|\|\hat{\epsilon}\|\|\|$	2.3234	1.8924	1.2509	0.7153	0.3738
J^-	-16.8051	-3.3567	3.3228	5.4447	6.0829
J^+	34.6587	17.1489	9.3096	7.0083	6.4621

APPENDIX

We prove here the expression (11) and provide an upper bound for the value of the constant η. For the two dimensional case of interest here, the stress and deformation tensors only have three independent components. Therefore, if we define the vectors $\underline{\boldsymbol{\sigma}} = \{\sigma_{11}, \sigma_{22}, \sigma_{12}\}^T$ and $\underline{\boldsymbol{\varepsilon}} = \{\varepsilon_{11}, \varepsilon_{22}, 2\varepsilon_{12}\}^T$, then, we have that

$$\underline{\boldsymbol{\sigma}} = \boldsymbol{D}\underline{\boldsymbol{\varepsilon}},$$

where $\boldsymbol{D}$ is the matrix of elastic coefficients

$$\boldsymbol{D} = \begin{bmatrix} \kappa + \frac{4}{3}\mu & \kappa - \frac{2}{3}\mu & 0 \\ \kappa - \frac{2}{3}\mu & \kappa + \frac{4}{3}\mu & 0 \\ 0 & 0 & \mu \end{bmatrix}$$

where μ is the shear modulus and κ is the bulk modulus as defined in section III. Let

$$\underline{\boldsymbol{v}}_{\boldsymbol{x}} = \left\{ \frac{\partial v_1}{\partial x_1}, \frac{\partial v_2}{\partial x_1}, \frac{\partial v_1}{\partial x_1}, \frac{\partial v_2}{\partial x_2} \right\}^T,$$

then, for a given displacement field $\boldsymbol{v} \in X$, we have

$$\underline{\boldsymbol{\varepsilon}} = \begin{bmatrix} 1 & 0 & 0 & 0 \\ 0 & 0 & 0 & 1 \\ 0 & 1 & 1 & 0 \end{bmatrix} \underline{\boldsymbol{v}}_{\boldsymbol{x}},$$

$$\underline{\boldsymbol{\sigma}} = \begin{bmatrix} \kappa + \frac{4}{3}\mu & 0 & 0 & \kappa - \frac{2}{3}\mu \\ \kappa - \frac{2}{3}\mu & 0 & 0 & \kappa + \frac{4}{3}\mu \\ 0 & \mu & \mu & 0 \end{bmatrix} \underline{\boldsymbol{v}}_{\boldsymbol{x}}\ , \tag{41}$$

and

$$W^e = \frac{1}{2}\underline{\boldsymbol{\sigma}}^T \cdot \underline{\boldsymbol{\varepsilon}} = \frac{1}{2}\underline{\boldsymbol{v}}_{\boldsymbol{x}}^T \tilde{\boldsymbol{D}}\, \underline{\overline{\boldsymbol{v}}}\boldsymbol{x}\ . \tag{42}$$

Here, $\tilde{\boldsymbol{D}}$ is given by

$$\tilde{\boldsymbol{D}} = \begin{bmatrix} \kappa + \frac{4}{3}\mu & 0 & 0 & \kappa - \frac{2}{3}\mu \\ 0 & \mu & \mu & 0 \\ 0 & \mu & \mu & 0 \\ \kappa - \frac{2}{3}\mu & 0 & 0 & \kappa + \frac{4}{3}\mu \end{bmatrix}\ .$$

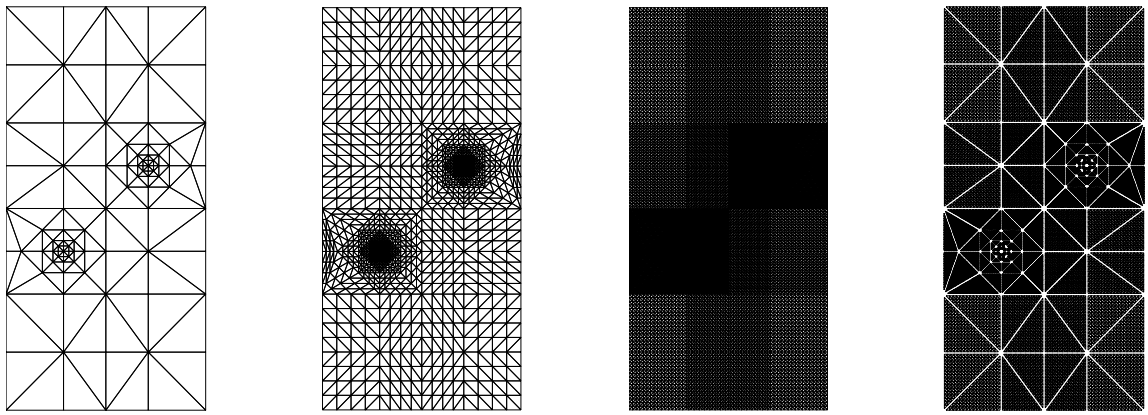

(a) (b) (c) (d)

Fig. 7. Finite element meshes used for open crack problem: (a) coarse mesh $\mathcal{T}_H$, (b) medium mesh $\mathcal{T}_{H/4}$, (c) fine mesh $\mathcal{T}_{H/16}$, and (d) illustration of broken mesh used for local problem solution associated to coarse mesh $\mathcal{T}_H$ (actual mesh is twice as fine e.g. $H/32$).

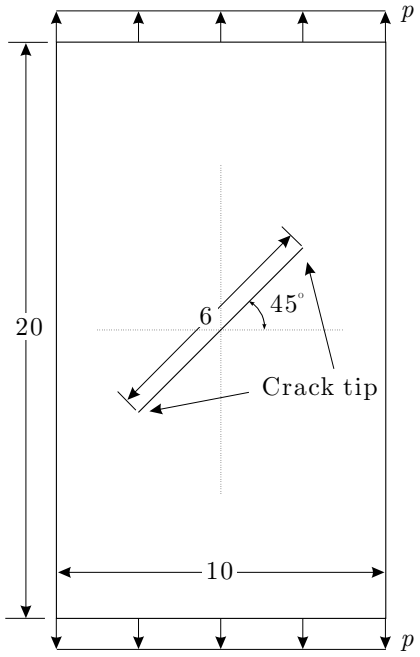

Fig. 5. Geometry of plate with an inclined crack subjected to a uniform tensile stress.

The quadratic terms in (7) can now be expressed as

$$(\boldsymbol{\nabla}\chi)^T \cdot \boldsymbol{\sigma}(\boldsymbol{v}) \frac{\partial \boldsymbol{v}}{\partial x_1} = \frac{1}{2} \underline{\boldsymbol{v}}_{\boldsymbol{x}}^T \boldsymbol{Q}\, \overline{\boldsymbol{v}}\boldsymbol{x},$$

where

$$\boldsymbol{Q} = \begin{bmatrix} 2(\kappa+\frac{4}{3}\mu)\frac{\partial\chi}{\partial x} & (\kappa+\frac{1}{3}\mu)\frac{\partial\chi}{\partial y} & \mu\frac{\partial\chi}{\partial y} & (\kappa-\frac{2}{3}\mu)\frac{\partial\chi}{\partial x} \\ (\kappa+\frac{1}{3}\mu)\frac{\partial\chi}{\partial y} & 2\mu\frac{\partial\chi}{\partial x} & \mu\frac{\partial\chi}{\partial x} & (\kappa+\frac{4}{3}\mu)\frac{\partial\chi}{\partial y} \\ \mu\frac{\partial\chi}{\partial y} & \mu\frac{\partial\chi}{\partial x} & 0 & 0 \\ (\kappa-\frac{2}{3}\mu)\frac{\partial\chi}{\partial x} & (\kappa+\frac{4}{3}\mu)\frac{\partial\chi}{\partial y} & 0 & 0 \end{bmatrix},$$

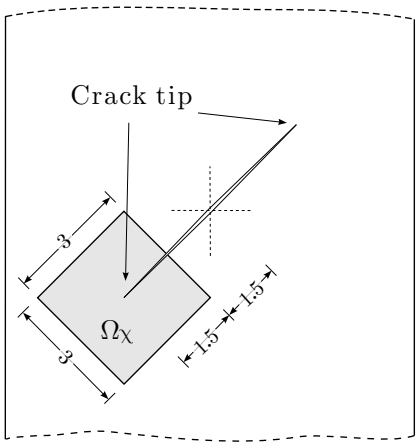

Fig. 6. Support of weighting function χ for the evaluation of the J-integral.

and

$$W^e \frac{\partial \chi}{\partial x_1} = \frac{1}{2} \underline{\boldsymbol{v}}_{\boldsymbol{x}}^T \left\{ \frac{\partial \chi}{\partial x_1} \tilde{\boldsymbol{D}} \right\} \underline{\boldsymbol{v}}_{\boldsymbol{x}}.$$

Then, $q(\boldsymbol{v},\boldsymbol{v})$ can be written as

$$q(\boldsymbol{v},\boldsymbol{v}) = \frac{1}{2} \int_{\Omega_\chi} \underline{\boldsymbol{v}}_{\boldsymbol{x}}^T \left[\boldsymbol{Q} - \frac{\partial \chi}{\partial x_1} \tilde{\boldsymbol{D}} \right] \underline{\boldsymbol{v}}_{\boldsymbol{x}} \mathrm{d}\Omega \ ,$$

and $|||\boldsymbol{v}|||^2$, is given by

$$a(\boldsymbol{v},\boldsymbol{v}) = \int_\Omega \underline{\boldsymbol{v}}_{\boldsymbol{x}}^T \tilde{\boldsymbol{D}}\, \overline{\boldsymbol{v}}\boldsymbol{x} \mathrm{d}\Omega \geq \int_{\Omega_\chi} \underline{\boldsymbol{v}}_{\boldsymbol{x}}^T \tilde{\boldsymbol{D}}\, \overline{\boldsymbol{v}}\boldsymbol{x} \mathrm{d}\Omega \ .$$

If we consider now the symmetric generalized eigenvalue problem,

$$\left(\boldsymbol{Q} - \frac{\partial \chi}{\partial x_1} \tilde{\boldsymbol{D}} - 2\lambda \tilde{\boldsymbol{D}} \right) \underline{\boldsymbol{v}}_{\boldsymbol{x}} = \boldsymbol{0} \ , \tag{43}$$

it is clear that if we choose $\eta = \max\{\lambda_1, \lambda_2, \lambda_3, \lambda_4\}$ then,

$$q(\boldsymbol{v},\boldsymbol{v}) \leq \eta a(\boldsymbol{v},\boldsymbol{v}), \tag{44}$$

as required. The eigenvalues of (43) can be found explicitly with the help of a symbolic manipulation program and the final expression for η is given in (19). We note that the value of η thus computed depends on $\boldsymbol{\nabla}\chi$. In our context, χ is chosen to be piecewise linear on $\mathcal{T}_H$, in which case $\boldsymbol{\nabla}\chi$ is piecewise constant. In order to determine the appropriate value for η we simply take the maximum over all the elements in $\mathcal{T}_H$.

REFERENCES

[1] M. Ainsworth, J.T. Oden, A posteriori error estimation in finite element analysis, Computer Methods in Applied Mechanics and Engineering, 142 (1997) 1-88.

[2] R.E. Bank and A. Weiser, Some a posteriori error estimators for elliptic partial differential equations, Mathematics of Computation, 44 (1985), 283-301.

[3] J.D. Eshelby, The energy momentum tensor in continuum mechanics, In Inelastic Behavior of Solids (Edited by M.F. Kanninen et al.), 77-114, McGraw-Hill, New York (1970).

[4] P. Heintz, F. Larsson, P. hansbo and K. Runesson, Adaptive strategies and error control for computing material forces in facture mechanics, Preprint 2002-18, Chalmers Finite Element Center, Chalmers Univeristy of Technology, 2002.

[5] P. Heintz, K. Samuelsson, On adaptive strategies and error control in fracture mechanics, Preprint 2002-14, Chalmers Finite Element Center, Chalmers Univeristy of Technology, 2002.

[6] F.Z. Li, C.F. Shih and A. Needleman, A comparison of methods for calculating energy release rates, Engineering Fracture Mechanics, 21 (1985) 405-421.

[7] S.H. Lo, C.K. Lee, Solving crack problems by an adaptive refinement procedure, Engineering Fracture Mechanics, 43 (1992) 147-163.

[8] K.S.R.K. Murthy and M. Mukhopadhyay, Adaptive finite element analysisi of mixed-mode fracture problems containing multiple crack-tips with an automatic mesh generator, Interantional Journal of Fracture 108: 251-274, 2001.

[9] M. Paraschivoiu, J. Peraire, A.T. Patera, A posteriori finite element bounds for linear-functional outputs of elliptic partial differential equations, Computer Methods in Applied Mechanics and Engineering. 150 (1997) 289-312.

[10] N. Pares, J. Bonet, A. Huerta and J. Peraire, Guaranteed bounds for outputs of interest in linear elasticity, submitted to Comp. Meth. for Appl. Mech. and Engrg., 2003.

[11] A.T. Patera and J. Peraire, A general Lagrangian formulation for the computation of a-posteriori finite element bounds', chapter in "Error Estimation and Adaptive Discretization Methods in CFD", Eds: T. Barth & H. Deconinck, Lecture Notes in Computational Science and Engineering, Vol. 25, 2002.

[12] J. Peraire, A.T. Patera, Bounds for linear-functional outputs of coercive partial differential equations: Local indicators and adaptive refinement, Proceedings of the Workshop On New Advances in Adaptive Computational Methods in Mechanics, edited by P. Ladeveze and J.T. Oden, Elsevier 1998.

[13] J.R. Rice, A path independent integral and approximate analysis of strain concentration by notches and cracks, Journal of Applied Mechanics, 35 (1968) 379-386.

[14] M. Ruter, E. Stein, Goal-oriented a posteriori error estimates in elastic fracture mechanics, Fifth World Congress on Computational mechanics, Vienna, Austria, July, 2002.

[15] A.M. Sauer-Budge, J. Bonet, A. Huerta and J. Peraire, Computing bounds for linear outputs of exact weak solutions to Poisson's equation, submitted to SINUM, March 2003.

[16] B.A. Szabo, Estimation and control of error based on p convergence, chapter 3 in Accuracy Estimates and Adaptive Refinements in Finite Element Computations, edited by I. Babuška, O.C. Zienkiewicz, J. Gago and E.R. de A. Oliveira, 1986, John Wiley.